Proceedings of 2016 IEEE
International Conference on Mechatronics and Automation
August 7 - 10, Harbin, China

Vision Based Embedded Tiny Spur Gear Inspection and Measurement System

Yibin Huang, Jiaojiao Gu, Shijun Wang, Han Xiao and Kui Yuan
Institute of Automation, Chinese Academy of Sciences, University of Chinese Academy of Sciences
95 Zhongguancun East Road, Beijing, China
Huangyibin2014@ia.ac.cn

***Abstract* – The machine vision based inspection and measurement system obtains more significant advantages, such as higher speed and accuracy. A vision based embedded tiny spur gear inspection and measurement system is proposed. The system, which is designed for measuring gear's addendum and dedendum diameter, and inspecting the tooth deformation. In this system, Field-Programmable Gate Array (FPGA) is used to extract the gear center and edge, and to conduct other image preprocessing. Digital Signal Processor (DSP) analyzes edge image to measure gear's diameter, and matches its contour to the designed diagram. The embedded vision system is real-time, small-size, non-contact, high-accuracy, high-speed, low-cost and low power consumption.**

Index Terms – Gear, Image process, Machine Vision, Inspection and Measurement, Embedded System.

I. Introduction

Gears are widely applied into industrial productions, delivering power and motion. There are a number of defects in finished gear products, such as broken tooth, askew tooth, burrs, out of size, large pitch error, which make the gear measurement and inspection more complicated. The quality of tiny spur gears is the guarantee for instrument's accuracy. A gear with those defects might cause more noise and wear, and affects the performance and service life of the equipment.

In most cases, inspectors use the microscope to monitor gear's quality with the method of human eyes recognition, which is high-cost but low-accuracy and low-efficiency. There are other massive solutions. For example, they exploit a probe to trace the contour of gear to examine whether it meets the requirements for the designed profile. These contact inspection systems are not suitable for tiny gears, and specialized instruments are expensive. A non-contact, lower-cost and more efficient solution is thus in demand.

The machine vision is cut out for measuring tiny spur gears, though this inspection technology is in its infancy. A camera equipped with a Personal Computer (PC) or a high performance development board, computer vision system is capable of inspecting several parameters and objects that are in one frame within one second. Simultaneously, it records, analyzes and distinguishes whether these products are substandard. However, some researchers have shown their concern about this method inspecting and measuring gears. For instance, D. Hongru et al., the research members from Lanzhou University of Technology, utilized a Charge-Coupled Device (CCD) sensor and MATLAB image toolbox to obtain gear's key parameters, such as addendum diameter, dedendum diameter, and the number of teeth [1]; MD. Hazrat Ali et al. from Kyushu University come up with a vision based inspection system to record video for the measuring accuracy of gear, mainly for surface error measurement [2]. Also, there are other works that employs computer vision [3-5], but all of them are carried out by computers rather than embedded systems.

High speed, small size, low power, low cost are the advantages of embedded vision systems. This paper takes aim at the real-time embedded vision system for tiny gears inspection and measurement.

II. Hardware System

In Fig.1, the hardware system consists of several parts, part ① is a universal platform to fix the camera and the development board; part ② is the Back-Light Compensation(BLC), with a LED light source to reduce the interference of changes in illumination condition. Part ③ is the lens and CCD camera. CCD image sensor will transmit images via a cable to the FD6000 image processing board (part ④) developed by our lab [6]. All of the image process and vision inspection algorithms are developed on this development board. Plug in the power, the board can work automatically, and the image frames and analysis results will be delivered to Advanced RISC Machine (ARM) or PC via a serial line or a network cable. Since most image processing programs apply FPGA's parallel acceleration technology, the time of inspection and measurement can be completed in milliseconds.

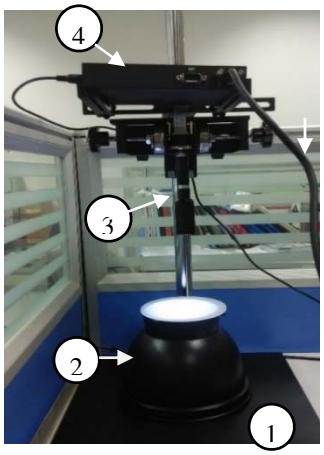

Fig. 1 Hardware of the vision system

FPGA and DSP are the major image processing elements. FPGA on the board is Altera's EP3C40F484C8, and DSP is TM320DM642 from TI (Texas Instruments). Logic elements of FPGA work as several parallel pipelines to process image, which is done as soon as the camera get a new frame. DSP enables FPGA to complete complex algorithms with its great addressing capacity. In addition, with 100M Ethernet, DSP delivers images and processing results to host computer, and receives instructions and parameters from it.

The CCD camera can work at a frame rate of 1/50, it means that the system can get 50 image frames of 640*480 resolution. The lens in used is MORITEX MML08-ST110 telecentric lens. A telecentric lens excels in many aspects. For instance, it has high performance magnifying tiny objects, high image resolution, near-zero deformation, zero perspective error, and large depth of field. MML08-ST11's resolution is 13.5μm, whose depth of field is 2.00mm and distortion only 0.002%.

As shown in Fig. 2, we took two photos of a radius of 195μm small hole respectively via an ordinary and a telecentric lens. The excellent image quality of telecentric lens is rather obvious. Combining with sub-pixel technology, the system has very high accuracy.

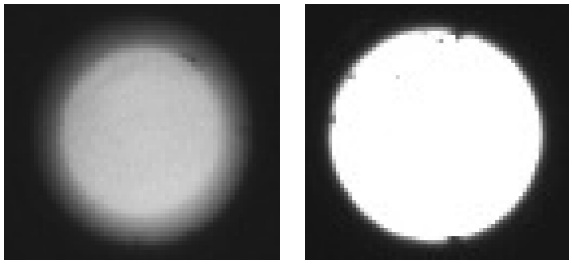

(a)Result of ordinary lens (b)Result of telecentric lens

Fig. 2 Results of different lens

III. IMAGE PROCESSING

Gears are core components of a mechanical watch, in which their quality will assure its time accuracy. The gear in Fig. 3 is a second gear (a gear that drives the second hand of a watch) is far smaller than a Chinese dime. Inspecting a same-size gear might brush up against obstacles. Considering the cost, manufacturers will not hire inspectors to make sure all gears are qualified before assembling watch, which makes defective rate increase significantly. All gears used in experiments are second gears from a watch manufacturer.

Fig. 3 Gear's size compare with a coin

A. Image Segmentation

Binarization is a very simple but practical image segmentation method. The image of gears acquired from the CCD camera is a grayscale image. As we can see in Fig. 4, the background and foreground of the grayscale image are very clean and simple, and the histogram of the image is a typical dual peak and single trough model, so that global threshold(or mode method)[7] is an favorable threshold selection algorithm. This algorithm picks up the grayscale of the local minima between the two peaks in the histogram as the binarization threshold. As seen in Fig. 4 (a), high brightness area in the image is the background, at the histogram(Fig. 4 (b)), high brightness peak appeared at a gray level around 229; the dark area corresponds to the foreground, and its peaks in the histogram show up around 16, the local minima in the two peaks is about 120. We take this value as segmentation threshold, and obtain a pretty good segmentation results, the binary can be seen at Fig.5 (a).

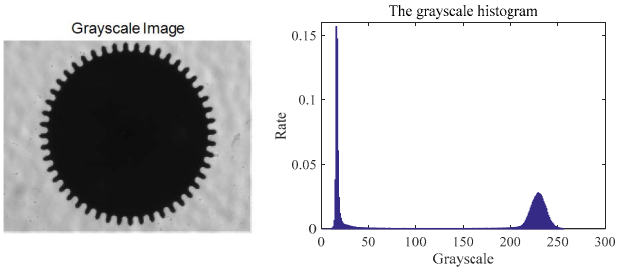

(a)Gear image (b)Histogram of the gear image

Fig. 4 Gear image and its grayscale histogram

B. Edge extraction

Since the important items of the gear measurement and inspection are all based on the contour of the gear, it is very critical to extract the edge of one pixel width. The edge extraction is based on four neighbor judgement [8], if a certain pixel in the binary image is black, and if its four neighborhood (left, right, up, down) has not less than one pixel is white, then label the pixel as edge; else, it is background. The algorithm can be described as follows:

If $B(x, y) == 0$ && $(B(x\text{-}1, y)+B(x+1, y)+ B(x, y+1)+ B(x, y\text{-}1)) > 0$

Mark the pixel at (x, y) as *Edge*

Else

Mark the pixel at(x, y) as *Background*

Where (x, y) is the coordinate of the pixel, $B(x, y)$ represents the pixel value in the binary image, 0 stands for black and 1 for white. In the edge image, the white pixels are edge and the black are background. The result is revealed at Fig. 5(b).

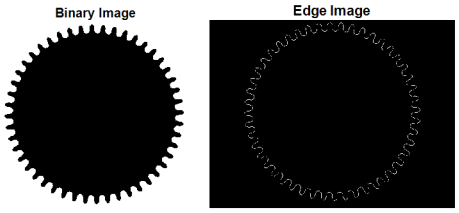

(a)Binary image (b)Edge of the gear

Fig. 5 Binary image and edge image of the gear

In Fig.5 (b) we can see that, the edge extraction algorithm can extract the gear's contour that is almost one pixel width. There are some special positions where more than one pixel on the contour are complied with the judgment that makes the edge width thicker than one pixel. Fig. 6 (a) is part of the edge image of the second gear. The edge still has few positions thicker than one pixel, and these noises will affect the accuracy of subsequent inspection and measurement. So the following edge thinning process is necessary. Fig.7 reveals four kinds of situations that the thinning process focus on, the pixel right in the middle is the current pixel, white stands for the pixels' label is 1 (edge) and gray means that those pixels we do not care about. Scan all pixels in the edge image, and checkup their four neighborhood, if the current pixel label is 1 (edge), and its four neighborhood meets any situations described in Fig. 7, the current point is marked as the background, else we don't change the label in the edge image.

This process can effectively eliminate the noises in the contours, Fig. 6 (b) is the edge after thinning.

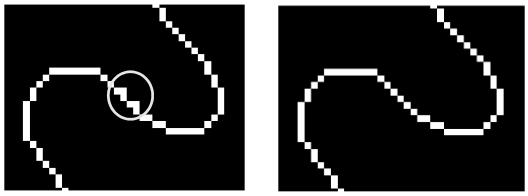

(a)Edge image (b)Thin edge image

Fig. 6 Edge image before and after thinning process

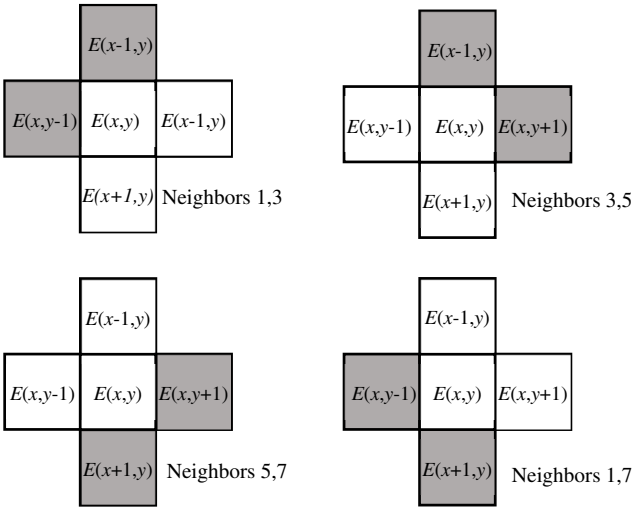

Fig.7 Situations that the thinning process focus on

C. Thick Edge Image Generation

A 3 pixels width edge image is needed in subsequent inspection algorithm. This so called thick image can be refined from morphological dilating the thin edge image. Scan the edge image with a 3 * 3 pixels template, then there always 9 pixels are covered by the template. If at least 1 of their label is 1 (edge), then mark the same pixel in thick edge image as 1, else, mark it as 0. The algorithm code can be described as follows:

If $E(x, y) + E(x-1, y) + E(x+1, y) + E(x, y+1) + E(x, y-1) + E(x-1, y-1) + E(x-1, y+1) + E(x+1, y+1) + E(x+1, y-1) > 0$

Mark the pixel at (x, y) as thick edge

Else

Mark the pixel at (x, y) as background

$E(x, y)$ is the label of the pixel at (x, y) in the edge image, the label has only two values, which 1 stands for "edge" while 0 stands for "background" . Then we got the thick image shown in Fig. 8(b).

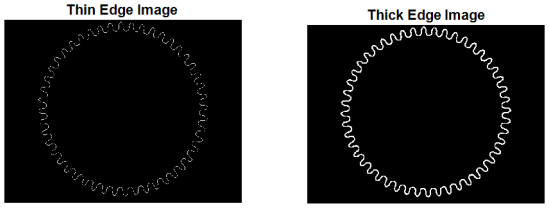

(a) Thin edge image (b) Thick edge image

Fig. 8 Edge thicken process

IV. MEASUREMENT AND INSPECTION

In this paper, the gears in use are the second gears of a certain kind of watches, and the main measurement and inspection items are addendum circle diameter, dedendum circle diameter and tooth deformation. After calibration, we know that 1 pixel in the image represents 7.62 μm, assist with the sub-pixel technology, the process of measurement can precision to sub-pixel level. So this system will be very suitable for measurement and inspection the second gears. Because the directions of the gears in the image are variable, the measurement and inspection algorithms need direction invariance.

A. Gear Center Detection

Identifying the location of the gear center is crucial because the design of spur gear has a strict requirement for central symmetry. The accuracy of center position is directly related to the subsequent measurement and inspection algorithms. Template matching and the center of gravity are the commonly used center detection methods. The idea of template matching is using a standard template to scan the image, finding the location where the similarity is higher than a certain threshold, then storing them in candidates list, finally using candidates gravity center as gear center [9]. Experiments verify

that the maximum error of this center detection method is 1-2 pixels, such a large error will seriously affect the accuracy of the system. Template matching method also takes up too many FPGA resources, and its hardware code is too long. We thus choose the gravity method. Equation (1) and (2) show how to apply gravity method to locate the center. X_c is the center's x coordinate, x_i *is* x coordinate of the i-th foreground pixel, n is the number of pixels of the foreground. And Y_c can be calculated in the same way. Precision of barycenter algorithms is much higher, the error is far smaller than one pixel. We keep one decimal place as the sub-pixel level accuracy center location.

$$X_c = \frac{1}{n}\sum_{i=1}^{n} x_i \tag{1}$$

$$Y_c = \frac{1}{n}\sum_{i=1}^{n} y_i \tag{2}$$

B. Diameter Measurement

In Fig.9, we take gear center (X_c, Y_c) as a coordinate origin to build a coordinate system. Knowing a pixel's location (x, y), we calculate the pixel's angle θ and distance ρ with trigonometric functions. While in another coordinate system, we use θ as the horizontal axis and ρ as the vertical one. The gear, from this perspective, will be as well as Fig. 10. Thus, the gear teeth contours will be a periodic curve. We then carry out a further work.

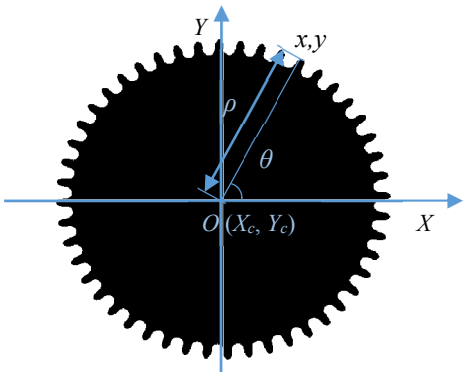

Fig. 9 Polar coordinate system of the gear

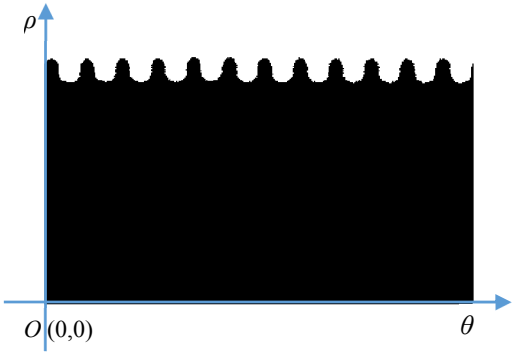

Fig. 10 Polar transformation result of the gear

The second gear has 48 teeth, thus the angle of each tooth is 7°30′.We set the angle resolution to 9′, in Fig. 9 the angle of half-line O-X is 0°0′, counterclockwise move around the origin O, the angle is divided into 2400 parts, the continuous value will approximate to discrete value among 0, 9′, 18′, ..., 359°51′. This discretization is necessary in order to reduce computational cost.

In fact the polar coordinate system we describe above is built on the thin edge image. We calculate each edge pixel's θ and ρ, then we get an "average tooth". The algorithm can be described as equation (3) - (8).

$$X_i = X_i^{edge} - X_c \tag{3}$$

$$Y_i = Y_i^{edge} - Y_c \tag{4}$$

$$\rho_i = \sqrt{X_i^{\,2} + Y_i^{\,2}} \tag{5}$$

$$\theta_i = \begin{cases} \arcsin(Y_i/\rho_i) & when \quad X_i >= 0 \; and \; Y_i >= 0 \\ 360 + \arcsin(Y_i/\rho_i) & when \quad X_i >= 0 \; and \; Y_i < 0 \\ 180 - \arcsin(Y_i/\rho_i) & when \quad X_i < 0 \end{cases} \tag{6}$$

$$k_i = \begin{cases} round\left(\dfrac{\theta_i - 7.5 * floor(\theta_i / 7.5)}{0.015}\right) & when\ k_i < 50 \\ 0 & when\ k_i = 50 \end{cases} \tag{7}$$

$$AverageGear[j] = \frac{\sum_{i=1}^{n} \delta(k_i - j)\rho_i}{\sum_{i=1}^{n} \delta(k_i - j)}, \quad j = 1,2,...,50 \tag{8}$$

In equation (8), the array called *AverageTooth* which stores the average ρ of the 48 teeth. δ is Dirac function, it is well known that $\delta(0)=1$ and $\delta(x)=0 \; when \; x!=0$. In equation (3) - (8) X_i^{edge} is x coordinate the i-th edge pixel in the thin edge image and Y_i^{edge} is y coordinate; ρ_i is the distance between edge to the gear center. So the *AverageTooth* record the relationship between the angle θ and the distance ρ. If there is any tooth, the relationship between angle and the distance is abnormal, the gear is a defective product.

Take the maximum value of the average tooth, we take it as the addendum circle radius, and the minimum value as the dedendum circle radius. The diameter and the direction of the gear can be estimated as follows:

$$D_{addenum} = 2 * \underset{0<=j<50}{Max}(AverageTooth[j]) \tag{9}$$

$$D_{dedenum} = 2 * \underset{0<=j<50}{Min}(AverageTooth[j]) \tag{10}$$

$$\sigma = \arg\underset{0<=j<50}{Max}(AverageTooth[j]) * 9' \tag{11}$$

$D_{addendum}$ and $D_{dedendum}$ is the diameter, their unit is pixel, and their accuracy is 0.5 pixels. If the gear rotate σ clockwise, one of the teeth will be point to the same direction with half-line O-X.

C. Tooth shape inspection

If we know the design of the gear, then we get the relationship between angle θ and distance ρ of the profile (or edge) of a standard tooth. So we match each tooth on the gear to the standard tooth, to see whether they are qualified. The inspection steps can be described as follows:

1) Create an array called *StandardTooth* to record the relationship between the angle θ and the distance ρ of a standard tooth;

2) Use σ, X_c, Y_c, and *StandardTooth* to draw a 1 pixel width gear edge image called standard gear;

3) Matching the standard gear image and the thick gear image;

4) Set an appropriate threshold and see whether all the teeth are qualified.

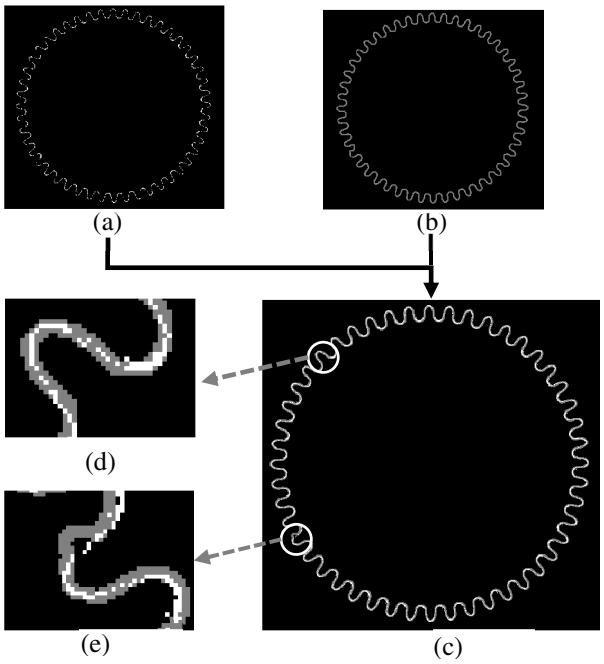

Fig.11 The matching process

This matching method is based on edge. The thin edge is the contour of the gear, and the thick edge means a neighbor area which is 1 pixel distance around the gear contours. That is to say, if there is any pixel on edge of the gear whose distance to the design contours is greater than or equal to 2 pixels, then this pixel will be detected. Of course, we can change the width of the thick edge according to the accuracy requirement of the design. Fig. 11 show the matching process, (a) is the "standard gear" image, (b) is the thick edge image, (c) shows the matching results, and (d)(e) is details of (c).

In this paper, the template *StandardTooth* stores 50 distance value, these value stands for 50 uniformly distributed pixels on a standard tooth's edge. In the "standard gear" image, those edge pixels are overlapped by thick edge will be called matched pixels. We count each tooth's matched pixels number M and calculate the matching rate R_i with equation (12).

$$R_i = \frac{M_i}{50}, i = 1, 2, ..., 48 \tag{12}$$

Considering that pitch deviation can't be ignored, the matching algorithm must be adaptive to the pitch deviation. As a result, if we find any evidence that the matching rate R is lower than the threshold, we move the template in an angle range. We take the highest matching rate as R_i. The angle range is within the maximum allowable cumulative pitch deviation $F_{p\varphi}$, $F_{p\varphi}$ can obtain by equation (14). F_p is also cumulative pitch deviation, F_p can be estimated with equation (13) with gear's model m and reference circle diameter d , check tables on ISO 1328:2013 or given by the gear designer. Fig. 12 shows that the 33th tooth has a low matching rate, it is the deformed tooth in Fig. 11 (e).

$$F_p = 0.3m + 1.25\sqrt{d} + 7 \tag{13}$$

$$F_{p\varphi} = \frac{206.246 * F_p}{d/2} \tag{14}$$

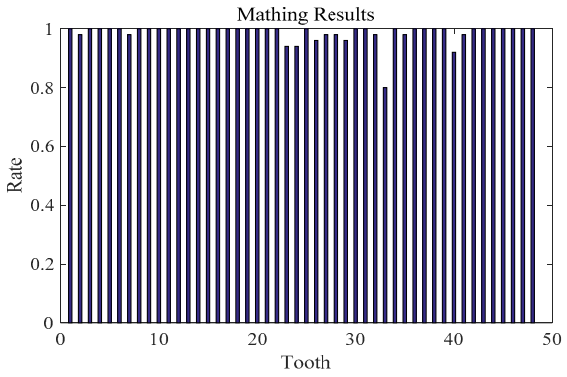

Fig.12 The matching rate of each tooth

V. IMPLEMENTED SYSTEM

One of the FPGA's advantages is the hardware parallel computing. There are a large number of operations in image processing, while parallel processing is supposed to have a high performance -- it can greatly compress the calculating time. In this paper, image binaryzation, edge extraction, center detection and other preprocessing shown in Fig.13 are implemented in FPGA. A crystal oscillator on the CCD camera provides a 27M clock, image delivering and processing is on this clock. The images are delivered to FPGA one pixel per clock serially. With shift registers, process modules get the current area for image preprocessing or feature extraction algorithm. If calculated by the CPU, these preprocessing need a lot of loop operations, and the processing time is proportional to the cycle times, but with the FPGA, it can be done at the same time the image delivered to the FPGA.

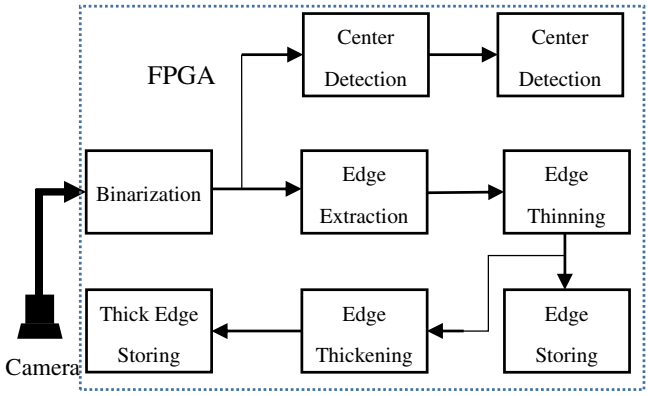

Fig.13 Image preprocessing in FPGA

When the thin edge image is generated, we save the coordinates of all the edge pixels rather than a binary image, and the number of the edge pixels is recorded. When calculating *AverageTooth*, we only need to run through the array. The result suggests that this method has higher processing efficiency and overcomes the weakness, such as endless loop or contours broken in Freeman chain-code contours tracking algorithm [10].

Coordinate transformation, diameter measurement and tooth matching are implemented in DSP. After accomplishing the step of sending processing results to PC host computer, the result of the gear measurement and inspection will be revealed as Fig. 14

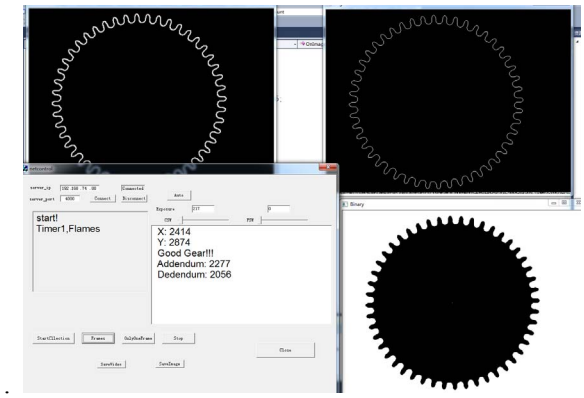

Fig.14 Monitoring software and results

VI. CONCLUSION

We put forward into a machine vision based tiny spur gear measurement and inspection system. Experiment results suggest that this system's accuracy of addendum and dedendum diameter measurement is capable of reaching 0.5 pixels. Larger than 2 pixels deformation will be count, and the gears will be classified by the deformation degree. All the algorithms are carried out through the FD6000 embedded development board. With FPGA hardware parallel acceleration technology, the maximum inspection speed is 20 frames per second. The system's characteristics, such as real-time, small-size, non-contact, high-accuracy, high-speed and low cost and low power consumption, will promote a higher performance.

ACKNOWLEDGMENT

This work is supported by the National Natural Science F oundation of China (No. 61273360).

REFERENCES

[1] D. Hongru, J. Wuyin, Z. Xia, and H. Jingping, "A Method of Dimension Measurement for Spur Gear Based On Machine Vision," In *Multimedia and Signal Processing (CMSP), 2011 International Conference* on (Vol. 1, pp. 243-246). IEEE.

[2] Ali, Md Hazrat, Satoru Kurokawa, and Kensuke Uesugi. "Vision based measurement system for gear profile." Informatics, Electronics & Vision (ICIEV), 2013 International Conference on. IEEE, 2013.

[3] S. Jun, "Study on Gear Chamfering Method based on Vision Measurement" International Conference on Informatization in Education, Management and Business (IEMB 2015) pp.145-149.

[4] Gadelmawla, E. S. "Computer vision algorithms for measurement and inspection of spur gears." *Measurement* 44.9(2011):1669-1678.

[5] L. Liang Yu, et al. "The Design of Vision Measurement System for Gear-appearance." *Machine Tool & Hydraulics*, 2004.

[6] G. Jiaojiao, et al. "A real-time small immobile object recognition system using wavelet moment invariants." Mechatronics and Automation (ICMA), 2015 IEEE International Conference on IEEE, 2015.

[7] Prewitt, Judith, and Mortimer L. Mendelsohn. "The analysis of cell images," *Annals of the New York Academy of Sciences* 128.3 (1966): 1035-1053.

[8] G. Liguo, "The inspection system research of small modulus plastic gear based on computer vision," Diss. Jilin University, 2007.

[9] G. Hao, et al. "Real-time detection and classification of machine parts with embedded system for industrial robot grasping." Mechatronics and Automation (ICMA), 2015 IEEE International Conference on. IEEE, 2015.

[10] Vaddi, R. S., et al. "Contour detection using freeman chain code and approximation methods for the real time object detection." *ASIAN JOURNAL OF COMPUTER SCIENCE & INFORMATION TECHNOLOGY* 1.1, 2013.